Arch Toxicol
DOI 10.1007/s00204-017-2056-0

INORGANIC COMPOUNDS

Early response of glutathione- and thioredoxin-dependent antioxidant defense systems to Tl(I)- and Tl(III)-mediated oxidative stress in adherent pheochromocytoma (PC12adh) cells

Lis C. Puga Molina[1] · Damiana M. Salvatierra Fréchou[2] · Sandra V. Verstraeten[2]

Received: 19 June 2017 / Accepted: 28 August 2017

Abstract Thallium (Tl) is a toxic heavy metal that causes oxidative stress both in vitro and in vivo. In this work, we evaluated the production of oxygen (ROS)- and nitrogen (RNS)-reactive species in adherent PC12 (PC12adh) cells exposed for 0.5–6 h to Tl(I) or Tl(III) (10–100 µM). In this system, Tl(I) induced mostly H_2O_2 generation while Tl(III) induced H_2O_2 and $ONOO^{-}$ generation. Both cations enhanced iNOS expression and activity, and decreased CuZnSOD expression but without affecting its activity. Tl(I) increased MnSOD expression and activity but Tl(III) decreased them. NADPH oxidase (NOX) activity remained unaffected throughout the period assessed. Oxidant levels returned to baseline values after 6 h of incubation, suggesting a response of the antioxidant defense system to the oxidative insult imposed by the cations. Tl also affected the glutathione-dependent system: while Tl(III) increased glutathione peroxidase (GPx) expression and activity, Tl(I) and Tl(III) decreased glutathione reductase (GR) expression. However, GR activity was mildly enhanced by Tl(III). Finally, thioredoxin-dependent system was evaluated. Only Tl(I) increased 2-Cys peroxiredoxins (2-Cys Prx) expression, although both cations increased their activity. Tl(I) increased cytosolic thioredoxin reductase (TrxR1) and decreased mitochondrial (TrxR2) expression. Tl(III) had a biphasic effect on TrxR1 expression and slightly increased TrxR2 expression. Despite of this, both cations increased total TrxR activity. Obtained results suggest that in Tl(I)-exposed PC12adh cells, there is an early response to oxidative stress mainly by GSH-dependent system while in Tl(III)-treated cells both GSH- and Trx-dependent systems are involved.

Keywords Thallium · Oxidative stress · Mitochondria · Antioxidant enzymes · Antioxidant defense system · Glutathione · Thioredoxin · PC12 cells

Abbreviations

Apocynin	4-Hydroxy-3-methoxyacetophenone
CAT	Catalase
CuZnSOD	CuZn-superoxide dismutase
DHE	Dihydroethidine
DHR123	Dihydrorhodamine 123
DMEM	Dulbecco's modified Eagle medium
DPI	Diphenylene-iodonium chloride
DTNB	Dithionitrobenzoic acid
GPx	Glutathione peroxidase
GR	Glutathione reductase
GSH	Glutathione
GSSG	Glutathione disulfide
iNOS	Inducible NOS
nNOS	Neuronal NOS
L-NAME	N^G-nitro-L-arginine methyl ester
mClBi	Monochlorobimane
MnSOD	Mn-superoxide dismutase
MTT	3-(4,5-Dimethylthiazol-2-yl)-2,5-diphenyl-tetrazolium bromide

Electronic supplementary material The online version of this article (doi:10.1007/s00204-017-2056-0) contains supplementary material, which is available to authorized users.

✉ Sandra V. Verstraeten
verstraeten@ffyb.uba.ar

[1] Instituto de Biología y Medicina Experimental (IBYME), Consejo Nacional de Investigaciones Científicas y Tecnológicas (CONICET), Buenos Aires, Argentina

[2] Universidad de Buenos Aires, Consejo Nacional de Investigaciones Científicas y Técnicas (CONICET), Instituto de Química y Fisicoquímica Biológicas (IQUIFIB), Facultad de Farmacia y Bioquímica, Buenos Aires, Argentina

Published online: 02 September 2017

NBT	2,2′-bis(4-Nitrophenyl)-5,5′-diphenyl-3,3′-(3,3′-dimethoxy-4,4′-diphenylene) ditetrazolium chloride
NOS	Nitric oxide synthase
NOX	NADPH oxidase
PBS	Phosphate buffered saline
PC12adh	PC12 cells, adherent variant
PI	Propidium iodide
Prx	Peroxiredoxin
RNS	Reactive nitrogen species
ROS	Reactive oxygen species
SDS	Sodium dodecyl sulfate
TrxR	Thioredoxin reductase

Introduction

Thallium (Tl) is heavy metal with no recognized biological functions, and considered by the USA Environmental Protection Agency (EPA) as a priority pollutant, along with lead, cadmium, and mercury. The most frequent routes of human intoxication with Tl are similar to those of other toxic metals, including the ingestion of Tl-containing compounds or the inhalation of air-borne particles and fumes (Repetto et al. 1998; ATSDR 1999; Peter and Viraraghavan 2005). Tl has two redox states, the monovalent [Tl(I)] and trivalent [Tl(III)] cations. Tl(I) is redox-inactive under biological conditions, but Tl(III) is a strong oxidant with high standard reduction potential ($\varepsilon^0 = +1.25$ V).

Based on its abundance and industrial applications, the investigation about Tl toxicity focused on Tl(I) rather on Tl(III), although the mechanisms involved are still not completely elucidated. Among other effects, Tl(I) accumulation induces an oxidative stress status. Galvan-Arzate and Rios (1994) found a positive association between the amount of Tl(I) in certain areas of rat brain and the content of lipid peroxidation products. In cultured rat pheochromocytoma (PC12) cells Tl(I) increases mitochondrial hydrogen peroxide (H_2O_2) production and decreases glutathione (GSH) levels (Hanzel and Verstraeten 2006). In addition, in human leukemia T (Jurkat) cells Tl(I) promotes lipid peroxidation that affects the biophysical properties of cell plasma membrane, both effects being prevented by cell pre-treatment with Trolox®, a water-soluble analog of vitamin E (Hanzel and Verstraeten 2006). Pourahmad et al. (2010) evidenced in cultured rat hepatocytes a relationship between Tl(I)-mediated alteration of cell redox status and the promotion of apoptosis. Tl(III) also increases cell oxidant production both in rat hepatocytes (Pourahmad et al. 2010) and PC12 cells (Hanzel and Verstraeten 2006; Pino et al. 2017). In both cellular models, GSH played a key role in the detoxification of the excess of oxidant species such as H_2O_2, and in the protection of the noxious effects of Tl(III) on cell integrity.

Usually, organisms respond to oxidative insults by modifying the activity and/or the expression of the enzymatic antioxidant defense system. The canonic system consists of the coordinated action of three enzymes: the superoxide dismutases (CuZnSOD and MnSOD) that dismutate superoxide anion ($O_2^{\cdot -}$) into H_2O_2 and O_2; catalase (CAT), that reduces H_2O_2 into O_2 and water; and glutathione peroxidase (GPx) that reduces H_2O_2 to water in a reaction coupled to GSH oxidation to GSSG. The latter is reduced back to GSH by glutathione reductase (GR), using NADPH as electron source, to keep an intracellular GSH to GSSG ratio ~10:1 (Halliwell and Gutteridge 1999; Wu et al. 2004). Both Tl(I) and Tl(III) interfere in vitro with this antioxidant defense system through the inhibition of GR and GPx (Villaverde et al. 2004). In addition, Tl(III) oxidizes GSH in vitro (Villaverde et al. 2004) which may contribute to cell oxidative damage. The participation of thioredoxin (Trx)-dependent system—comprised by the enzymes Trx, peroxiredoxin (Prx) and thioredoxin reductase (TrxR)—in the detoxification of diverse oxidants gained attention in the last decade (Hanschmann et al. 2013). Prx reduces H_2O_2 to water in a fast (Ogusucu et al. 2007; Manta et al. 2009), multistep process that involves the oxidative dimerization of Prx (Lu and Holmgren 2014). Prx is reduced by Trx, which is subsequently reduced by TrxR using NADPH as the electron source (Hanschmann et al. 2013). Prx is a very abundant protein—up to 1% of cell soluble proteins (Chae et al. 1999)—making Trx-dependent system a major antioxidant system. To the best of our knowledge, there are no studies about the effects of Tl on Trx-dependent system.

This work is an extension of our previous findings and was aimed to investigate if, similarly to the observed in the traditional PC12 cell line, low micromolar concentrations of Tl(I) or Tl(III) induce an oxidative stress status in the adherent variant (PC12adh cells), as a common mechanism of Tl toxicity. These cells were chosen because they can be differentiated in vitro to catecholaminergic neurons and constitute a well-accepted model for neurotoxicity studies (Wang et al. 2015). Even when PC12adh variant is an adaptation of traditional PC12 cells to enhance their adhesion, these cells have different morphology and duplication rate (Wang et al. 2015). On this basis, we evaluated first the kinetics and sources of Tl(I)- and Tl(III)-mediated oxidant species generation and next characterized the expression and activity of the enzymes responsible for their detoxification.

Materials and methods

Chemicals

Dulbecco's modified Eagle medium (DMEM high glucose) was purchased from Gibco BRL (Grand Island, NY,

USA). Donor horse serum was from PAA Laboratories GmbH (Pasching, Germany) and fetal bovine serum was from Natocor (Córdoba, Argentina). Thallium(I) nitrate was from Fluka (Milwaukee, WI, USA). Thallium(III) nitrate was from Alfa Æsar (Ward Hill, MA, USA). The following reagents: 3-(4,5-dimethyl-2-thiazolyl)-2,5-diphenyl-2*H*-tetrazolium bromide (MTT), poly-L-lysine hydrobromide, glutathione (GSH), glutathione disulfide (GSSG), 2,2′-bis(4-nitrophenyl)-5,5′-diphenyl-3,3′-(3,3′-dimethoxy-4,4′-diphenylene) ditetrazolium chloride (NBT), β-nicotinamide adenine dinucleotide 2′-phosphate reduced tetrasodium salt hydrate (NADPH), bovine erythrocyte superoxide dismutase (E.C. 1.15.1.1), thioredoxin from *E. coli* (E.C. 1.8.4.10), rat liver thioredoxin reductase (E.C. 1.8.1.9), bovine milk xantine oxidase (E.C. 1.1.3.22), dithionitrobenzoic acid (DTNB), sodium xanthine, bisbenzimide H (Hoechst 32258), propidium iodide (PI), N^G-nitro-L-arginine methyl ester (L-NAME), 4-hydroxy-3-methoxyacetophenone (apocynin), sulfanilic acid, *N*-(1-naphthyl)ethylene diamine (NEDA), the dyes Neutral red and Amido black, and all the other reagents had the highest quality available, and were from Sigma-Aldrich (St. Louis, MO, USA). Dihydrorhodamine 123 (DHR123), dihydroethidine (DHE) and monochlorobimane (mClBi) were from Invitrogen/Life Sciences (Grand Island, NY, USA). Diphenyleniodonium chloride (DPI) was from Calbiochem (La Jolla, CA, USA).

Primary antibodies against β-tubulin (sc-9104), actin (sc-1616), catalase (CAT; sc-34285), CuZn-superoxide dismutase (CuZnSOD; sc-11407), Mn-superoxide dismutase (MnSOD; sc-18504), glutathione peroxidase 1/2 (GPx1/2; sc-133160), glutathione reductase (GR; sc-133136), peroxiredoxin (Prx; sc-23969), inducible nitric oxide synthase (iNOS; sc-649) and neuronal NOS (nNOS; sc-5302) were from Santa Cruz Biotechnology (Santa Cruz, CA, USA). Primary polyclonal antibodies against thioredoxin reductase isoform 1 (TrxR1; ab16840) and isoform 2 (TrxR2; ab58445) were from Abcam (Cambridge, MA, USA). Horseradish peroxidase-conjugated secondary antibodies were from Jackson ImmunoResearch Inc. (West Grove, PA, USA). Complete, EDTA-free protease inhibitor cocktail was from Roche Diagnostics GmbH (Mannheim, Germany). PVDF membranes were from Bio-Rad Corp. (Hercules, CA, USA).

Tl solutions

Tl(I) and Tl(III) stock solutions were prepared as previously described (Hanzel and Verstraeten 2006). The amounts of Tl(I) or Tl(III) used in the experiments did not affect the pH of the culture medium.

Cell culture

Rat adrenal pheochromocytoma cells (PC12 cells, adherent variant; CRL-1721.1) were obtained from the American Type Culture Collection (A.T.C.C., Rockville, MD, USA), and cultured as described (Hanzel and Verstraeten 2006). These cells were adapted by the provider to enhance their adherence to plastic surfaces, and show differences with the parental cell line (Wang et al. 2015). As indicated for the individual experiments, cells were seeded on 100 mm Petri dishes (1×10^7 cells), or 96- or 48-well plates (3×10^4 and 5×10^5 cells/well, respectively) and allowed to grow until ~90% of confluence. Culture media were replaced, and cells were added with Tl(I) or Tl(III) (10–100 µM) and further incubated as indicated for the individual experiments.

Cell viability

Cells were grown on 96-well plates and incubated for 6 h in the conditions described above, and cell viability was evaluated by MTT reduction assay (Mosmann 1983; Hanzel and Verstraeten 2006). The absorbance of formazan was recorded at 570 nm (reference 620 nm) in a Rayto RT-2100C microplate reader (Rayto Life and Analytical Sciences Co., Shenzhen, P.R. China).

Alternatively, the viability of cells exposed to the inhibitors diphenylene iodonium (DPI) or apocynin, with or without Tl(I) or Tl(III), was assessed from Neutral red uptake (Pino et al. 2017).

Evaluation of mitochondrial oxidant content

Steady-state content of mitochondrial oxidants was evaluated as described previously (Hanzel and Verstraeten 2006). Cells were grown on clear-bottom 96-well plates apt for fluorescence measurements (Porvair Sciences Limited, Wales, UK) and incubated at 37 °C for 0.5–6 h in the presence of 10–100 µM Tl(I) or Tl(III). Alternatively, cells were preincubated for 30 min in the absence or presence of 100 µM DPI and subsequently exposed for 1 h to 10–100 µM Tl(I) or Tl(III). Samples were added with 50 µl of PBS containing 5 µM DHR123, incubated at 37 °C for 30 min, washed twice with warm PBS to eliminate non-incorporated probe, and disrupted with 0.1% (v/v) Igepal in PBS. Fluorescence emission was recorded at 535 nm ($\lambda_{excitation}$: 525 nm) in a top-reading PerkinElmer LS55 fluorometer (PerkinElmer Ltd., Beaconsfield, UK). Results were normalized by DNA content in the samples measured by reaction with 25 µM Hoechst 32258 ($\lambda_{excitation}$: 370 nm, $\lambda_{emission}$: 420 nm). Results were expressed as the ratio between DHR123 and Hoechst 32258 fluorescence intensities.

NADPH oxidase (NOX) activity

NOX activity was evaluated as described by Castilho et al. (1999). Cells were grown on clear-bottom 96-well plates apt for fluorescence measurements, pre-incubated for 30 min in the absence or presence of 100 µM apocynin, and exposed for 0.5–6 h to 10–100 µM Tl(I) or Tl(III). Culture media were discarded, and cells were washed twice with warm PBS and disrupted for 30 min at 37 °C with 0.1 ml of Igepal 0.1% (v/v). After the addition of 50 µl of a solution containing 0.3 mM dihydroethidine (DHE) and 1.5 mM NADPH in PBS, samples were incubated at 37 °C for 1 h and the fluorescence intensity was recorded at 634 nm ($\lambda_{excitation}$: 465 nm). Results were normalized by DNA content in the samples, as described above.

Evaluation of extracellular nitrite content

Cells were grown on 48-well plates and incubated for 6 h in the conditions described above. Culture media were separated and centrifuged at 800×*g* for 5 min, and nitrite content was evaluated in the supernatants (Guevara et al. 1998). The concentration of nitrite in the samples was calculated from a standard curve run in parallel, using freshly prepared sodium nitrite solution.

Evaluation of GSH content

Cells were grown on clear-bottom 96-well plates apt for fluorescence measurements and exposed to 10–100 µM Tl(I) or Tl(III) for 1–6 h. Cells were washed twice with warm PBS and added with 0.15 ml of 40 µM monochlorobimane (mClBi) in PBS (Hanzel and Verstraeten 2006). After 30 min of incubation at 37 °C, the fluorescence emission of the GSH-mClBi complex was recorded at 460 nm ($\lambda_{excitation}$: 395 nm). Cells were disrupted with 2% (v/v) Igepal, and DNA content in the samples was measured with 50 µM propidium iodide (PI) ($\lambda_{excitation}$: 538 nm, $\lambda_{emission}$: 590 nm). Results were expressed as the ratio between GSH-mClBi and PI fluorescence intensities.

Preparation of cell lysates

Cells were grown on 100 mm Petri dishes and exposed to 10–100 µM Tl(I) or Tl(III) for 6 h. Cells were washed twice with warm PBS, collected by scrapping, centrifuged at 800×*g* for 10 min at 4 °C and pellets were frozen at −80 °C for at least 1 h. Pellet rupture was completed by incubating samples for 30 min at 4 °C in buffer solutions suitable for either Western blot analysis [50 mM HEPES buffer (pH 7.4), 150 mM NaCl, 0.5 mM EDTA, 1% (v/v) Igepal, 1 mM PMSF, 5 mM DTT, and protease inhibitors] or enzyme activity determination [50 mM HEPES buffer (pH 7.4), 125 mM KCl and protease inhibitors]. Samples were centrifuged for 30 min at 10,000×*g* at 4 °C. Supernatants were separated, analyzed for protein content (Bradford 1976), divided into small aliquots to prevent the loss of enzyme activity by successive freeze/thaw cycles, and stored at –80 °C until their use.

Western blot analysis

Samples containing equal amounts of protein were separated by SDS-PAGE in gels containing 7.5% (w/v) (iNOS), 12.5% (w/v) (CAT, GR, TxrR1 and TxrR2) or 15% (w/v) (GPx, Prx, CuZnSOD and MnSOD) polyacrylamide, and transferred to PVDF membranes. Colored molecular weight standards (GE Healthcare, Piscataway, NJ, USA) were ran simultaneously. Membranes were blocked for 1 h in 2.5% (w/v) bovine serum albumin in Tris buffered saline containing 0.1% (v/v) Tween-20, and incubated overnight at 4 °C with the corresponding primary antibody. The following dilutions of antibodies were used: Prx and nNOS: 1:200; iNOS, CAT, GPx, MnSOD and CuZnSOD 1:500; GR, TrxR1, TrxR2, β-tubulin and actin 1:1000. Membranes were further incubated for 90 min with the corresponding peroxidase-conjugated secondary antibody (dilution 1:10,000). Specific bands were revealed with chemiluminescent Pierce® ECLplus Western blot substrate (Thermo Scientific, IL, USA) and detected using Amersham Hyperfilm ECL (GE Healthcare Bio-Sciences, PA, USA). Raw data were analyzed using the open-access software GelAnalyzer 2010a (http://www.gelanalyzer.com). Data were normalized by protein loading using β-tubulin or actin, as indicated for the individual experiments.

Antioxidant enzymes activities

CAT

CAT activity was estimated from the consumption of H_2O_2 (Johansson and Borg 1988). Briefly, 40 µl of cell lysates were added with 0.86 ml of 50 mM phosphate buffer (pH 7.4) and reaction was started by the addition of 0.1 ml of 0.06 M H_2O_2. CAT activity was calculated from the absorbance at 240 nm ($\varepsilon = 43.6\ M^{-1}\ cm^{-1}$) recorded for 2 min every 8 s. Results were expressed as µmol H_2O_2 consumed min^{-1} mg $protein^{-1}$.

GPx

GPx activity was estimated using FOX assay (Dringen et al. 1998; Villaverde et al. 2004). Briefly, 10 µl of cell lysates were added with 0.2 ml of 2 mM GSH, 0.5 mM cumene hydroperoxide, 1.5 mM EDTA and 1 mM sodium azide in 30 mM K_2HPO_4, 20 mM KH_2PO_4 buffer (pH 7.4).

Mixtures were incubated at 37 °C and every 5 min, 10 µl of the mixture were transferred to 96-well plates containing 0.1 ml of 10 mM sorbitol, 4 mM $FeSO_4$, 2 mM xylenol orange in 25 mM H_2SO_4. Samples were incubated for 45 min at room temperature and the absorbance at 560 nm was recorded. Cumene hydroperoxide remaining in the samples was estimated from a standard curve run in parallel. Results were expressed as µmol cumene hydroperoxide consumed min^{-1} mg $protein^{-1}$.

GR

GR activity was estimated as described by Villaverde et al. (2004) with modifications. Twenty microliters of cell lysates were added with 0.2 ml of a freshly prepared solution containing 62.5 mM GSSG, 0.15 mM NADPH, 0.1 M Na_2PO_4 buffer (pH 7.6) containing 0.5 mM EDTA. The fluorescence of NADPH at 460 nm ($\lambda_{excitation}$: 350 nm) was recorded for 10 min every 25 s. The amount of NADPH remaining in samples was estimated from a standard curve run in parallel. Results were expressed as µmol NADPH consumed min^{-1} mg $protein^{-1}$.

2-Cys Prx

Two-Cys Prx activity was estimated as described by Kim et al. (2005). Twenty µl of cell lysates were added with 0.180 ml of a freshly prepared solution containing 1 mM EDTA, 0.1 mM NADPH, 1.5 mM Trx, 100 mU TrxR in 50 mM HEPES buffer (pH 7.4). Reaction was started by addition of 0.476 mM H_2O_2 and the kinetics of NADPH oxidation were recorded every minute for 35 min at 460 nm ($\lambda_{excitation}$: 350 nm). Results were expressed nmol NADPH consumed min^{-1} mg $protein^{-1}$.

TrxR

TrxR activity was estimated using insulin as substrate (Holmgren and Bjornstedt 1995). Fifty µl of a freshly prepared solution containing 0.36 mM NADPH, 1.33 mM EDTA, 19 U ml^{-1} bovine insulin, 0.114 mg ml^{-1} Trx in 50 mM HEPES buffer (pH 7.4) were poured into 96-well plates. Reaction was started by adding 10 µl of cell lysates containing 30–50 µg protein, and samples were incubated at 37 °C for 20 min. Samples without added Trx were run in parallel (blanks). Reaction was stopped adding 0.24 ml of a solution containing 0.5 mM DTNB and 6 M guanidinium hydrochloride in 0.2 M Tris–HCl buffer (pH 8.0). TrxR-mediated TNB generation was measured at 412 nm (ε = 13,600 M^{-1} cm^{-1}). Results were expressed as µmol TNB.20 min^{-1} mg $protein^{-1}$.

SOD

SOD activity was estimated as described by Sun et al. (1988). For total SOD (CuZnSOD and MnSOD) activity, 25 µl of cell lysates were added to 1 ml of freshly prepared 0.1 mM EDTA, 50 µM xantine, 7 mU xantine oxidase, and 90 µM NBT in 50 mM K_2HPO_4 (pH 7.8). The absorbance of the samples was recorded at 560 nm for 1 min every 5 s. For MnSOD activity determination, CuZnSOD was inhibited previously with 2 mM KCN. CuZnSOD activity was estimated as the difference between total SOD and MnSOD activities.

Statistics

The effects of Tl(I) and Tl(III) were analyzed by one-way analysis of variance (ANOVA) followed by Fisher's protected least square difference test. The comparison between the effects of Tl(I) and Tl(III) was performed by two-way ANOVA followed by Holm-Sidak's multiple comparisons test. All statistical analyses, non-linear data fitting and correlations were performed using the routines available in GraphPad Prism version 6.00 for Windows, GraphPad Software (San Diego, CA, USA). A probability (P) value <0.05 was considered statistically significant. Results are presented as the mean ± SEM, and the number of independent experiments (n) is indicated in each figure legend.

Results

Effects of Tl on cell viability and oxidant species production

The effect of Tl on PC12adh cell viability was evaluated in cells exposed for 6 h to Tl(I) or Tl(III) (10–100 µM) from their capacity to metabolize the dye MTT. As reported previously (Hanzel and Verstraeten 2006), the effects of the cations on cell viability were negligible, with at least 95% of the cells being metabolically active (Suppl. Figure 1).

The kinetics of oxygen (ROS) and nitrogen (RNS) reactive species production in Tl-treated cells were investigated using the probe DHR123. Tl increases the steady-state level of mitochondrial H_2O_2 in parental PC12 cells (CRL-1721) (Hanzel and Verstraeten 2006). Because of the morphological and functional differences between PC12 and PC12adh cells (Wang et al. 2015), it was necessary to verify the effects of Tl(I) and Tl(III) in these cells. At 10 µM Tl(I) concentration, DHR123 oxidation increased linearly over time (Fig. 1a). At higher concentrations of Tl(I), the maximal

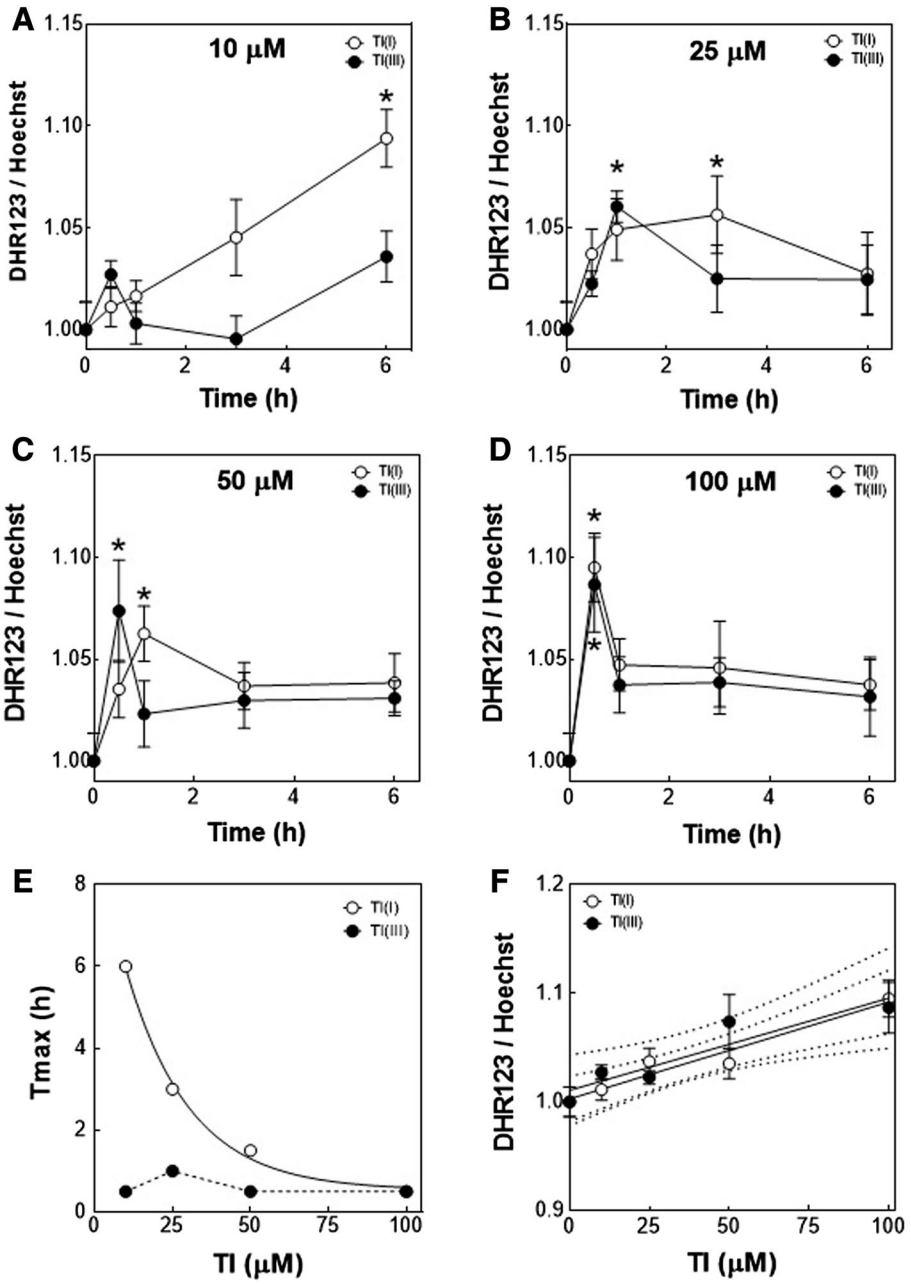

Fig. 1 Tl induced fast and transient oxidant production in PC12adh cells. PC12adh cells were incubated at 37 °C for 0.5–6 h in the presence of **a** 10 µM, **b** 25 µM, **c** 50 µM or **d** 100 µM Tl(I) (*open circle*) or Tl(III) (*filled circle*). ROS/RNS production was evaluated using the probe DHR123 and normalized by DNA content measured with Hoechst 32258. **e** Non-linear fitting of the incubation time necessary to achieve the maximal ROS production (T_{max}) in Tl(I) (*open circle*)-treated cells. No fitting was obtained for ROS production in Tl(III) (*filled circle*)-treated cells. **f** Correlation between ROS production after 0.5 h of cell exposure and Tl(I) (*open circle*) or Tl(III) (*filled circle*) concentration. Dotted lines show the 95% confidence band of the best fit-line. Results are shown as the mean ± SEM ($n = 3$). *Asterisk* denotes a statistical significance respect to the value measured in control cells ($P < 0.01$)

DHR123 oxidation moved towards the lower periods of incubation (Fig. 1b–d). Tl(III) caused a maximal effect between 0.5 and 1 h of incubation, regardless the concentration assessed (Fig. 1b–d). Once reached the maximal effect, DHR123 oxidation decreased toward a steady state value that was similar for all samples (Fig. 1b–d). The incubation time necessary to achieve maximal DHR123 oxidation (T_{max}) for each concentration of Tl(I) assessed can be described by the equation:

$$T_{max} = a \times e^{-k[Tl(I)]} + b,$$

where $a = 9.5$ h and $b = 0.4$ h, respectively, and $k = (0.053 \pm 0.004)\ \mu M^{-1}$ (Fig. 1e). A linear relationship was found between DHR123 oxidation measured at 30 min of incubation and cation concentration ($r^2 = 0.94$ and 0.87 for Tl(I) and Tl(III), respectively, $P < 0.001$) (Fig. 1f).

Both ROS and RNS oxidize DHR123, as evidenced in cells incubated with 500 µM H_2O_2 or 1 mM of NO donor S-nitrosoglutathione (GSNO) (Suppl. Figure 2). The source of oxidants in Tl-treated cells was next investigated. Cells preincubation for 30 min with 100 µM of flavoprotein inhibitor DPI, followed by exposure (without washing) for 1 h to Tl(I) or Tl(III) (10–100 µM), prevented Tl(I)- and Tl(III)-mediated DHR123 oxidation (Fig. 2a, b). Among other enzymes, DPI inhibits succinate dehydrogenase, which metabolizes MTT in mitochondria. Supporting that, MTT

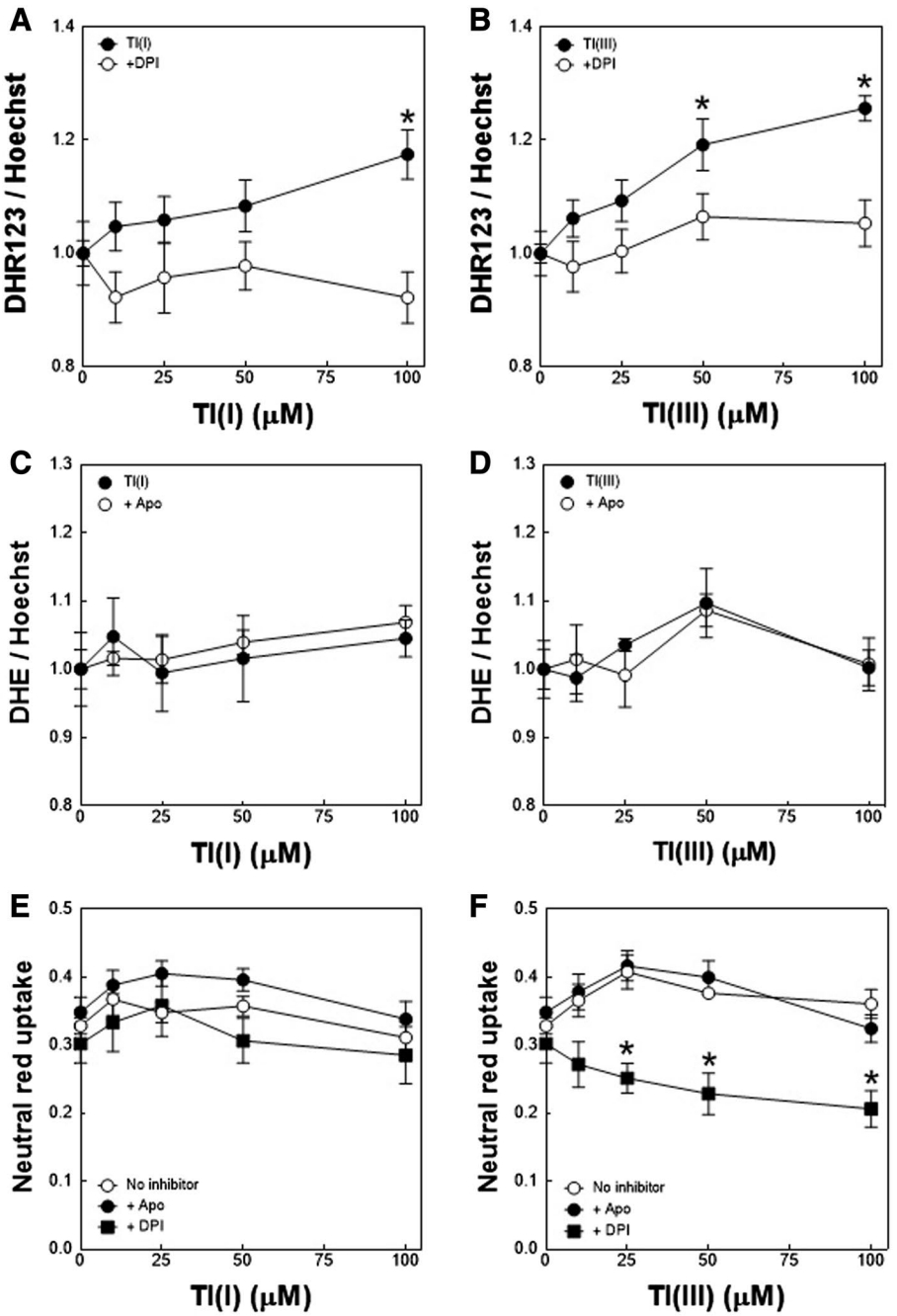

Fig. 2 Tl-induced oxidant production was mediated by flavoproteins different than NOX. The production of ROS and RNS was evaluated from DHR123 oxidation. DHR123-loaded PC12adh cells were pre-incubated at 37 °C for 30 min in the absence (*filled circle*) or presence (*open circle*) of 100 μM of DPI, and subsequently exposed for 1 h to **a** Tl(I) or **b** Tl(III) (10–100 μM). NOX activity was evaluated from DHE oxidation. DHE-loaded PC12adh cells were pre-incubated at 37 °C for 30 min in the absence (*filled circle*) or the presence (*open circle*) of 100 μM of NOX inhibitor apocynin (Apo), and then exposed for 1 h to **c** Tl(I) or **d** Tl(III) (10–100 μM). Results were normalized by DNA content measured with Hoechst 32258, and are shown as the mean ± SEM ($n > 3$). *Asterisk* denotes a statistical significance respect to the value measured in control cells ($P < 0.01$). PC12adh cells were incubated at 37 °C for 30 min in the absence (*open circle*) or presence of 100 μM DPI (*filled square*) or Apo (*filled circle*), and then exposed for 1 h to **e** Tl(I) or **f** Tl(III) (10–100 μM). Cell viability was evaluated from Neutral red uptake. Results are shown as the mean ± SEM ($n = 3$). *Asterisk* denotes a statistical significance respect to the value measured at the same Tl concentration but in the absence of inhibitors ($P < 0.01$)

metabolization in cells exposed to DPI was 60% lower than in the controls (Suppl. Figure 3), without being further affected by Tl(I) or Tl(III).

Another target of DPI is the plasma membrane-associated flavoprotein NOX, which generates $O_2^{\cdot-}$ and that is specifically inhibited by apocynin. NOX activity was evaluated using DHE, a probe specific for $O_2^{\cdot-}$ detection. Cells treated with 100 μM of pyrogallol were used as positive controls (Suppl. Figure 4). H_2O_2 (0.5 mM) also caused minor but significant DHE oxidation ($P < 0.01$ vs. control), the magnitude of its effects markedly lower than that of pyrogallol (Suppl. Figure 4). DHE oxidation in Tl-treated samples was comparable to that of the controls within the period assessed and not affected by apocynin, suggesting that the amount of H_2O_2 generated in Tl-treated samples was insufficient to oxidize DHE (Fig. 2c, d; Suppl. Figure 5).

Apocynin per se did not affect MTT metabolization, but cell co-incubation with Tl caused minor but significant decrease in this parameter (Suppl. Figure 1). Considering the limitations of MTT assessment, the uptake of vital dye Neutral red was also evaluated. Neither apocynin nor DPI affected Neutral red uptake in control (Fig. 2e,

f) or Tl(I)-treated cells (Fig. 2e). DPI, but not apocynin, decreased cell viability up to 30% in Tl(III)-treated cells (Fig. 2f). Thus, in DHR123 oxidation experiments, at least 70% of cells remained viable, in contrast to the observed from MTT assay (Suppl. Figure 3).

RNS generation was estimated from nitrite accumulation in the media. Both Tl(I) (Fig. 3a) and Tl(III) (Fig. 3b) increased nitrite content, reaching maximal effects at 50 and 25 μM, respectively. This effect was prevented by cell preincubation with L-NAME. Tl(I) and Tl(III) increased iNOS expression at similar concentrations ($P < 0.05$ vs. controls; Fig. 3c, d), but no nNOS expression was detected (data not shown). Significant correlations ($P < 0.01$) were found between iNOS expression after 6 h of cell exposure to Tl and nitrite content in the media (Fig. 3e, f).

Effects of Tl on the expression and activity of the main antioxidant enzymes

As DHR123 oxidation was restored to basal levels after 6 h of exposure to Tl (25–100 μM), we evaluated if this finding was related to increased expression and/or activity of the enzymes responsible for the removal of oxidant species.

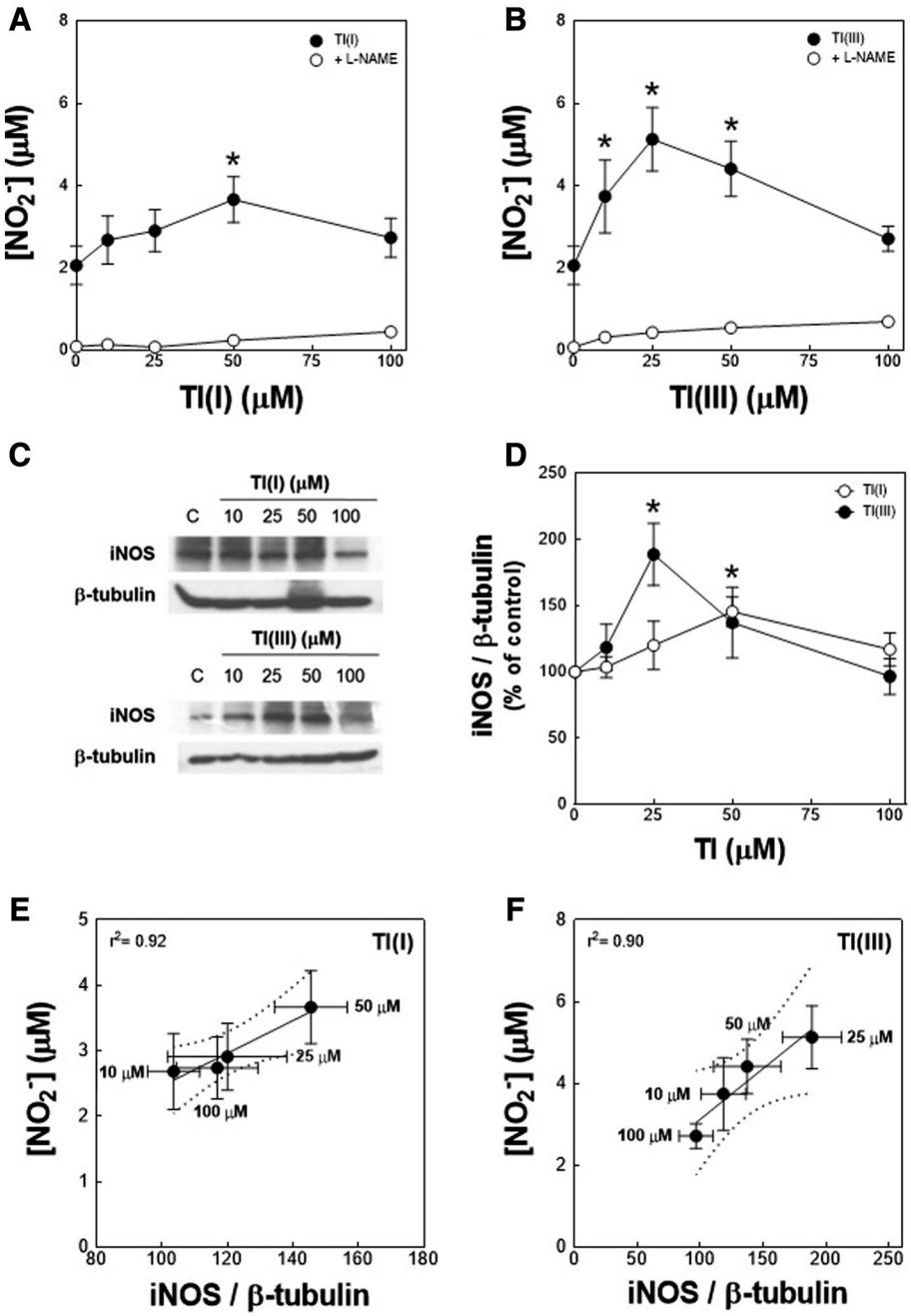

Fig. 3 Tl had a biphasic effect on iNOS expression and activity. PC12adh cells were preincubated at 37 °C for 1 h in the absence (*filled circle*) or presence of 1 mM L-NAME (*open circle*) and further incubated for 6 h in the presence of 10–100 μM **a** Tl(I) or **b** Tl(III). NO production was evaluated from nitrite content in the culture media. **c**, **d** Evaluation of iNOS expression. **c** Representative Western blots. **d** Quantification of iNOS to β-tubulin expression ratio in Tl(I) (*open circle*)- and Tl(III) (*filled circle*)-treated cells. Correlation between nitrite content in the culture media and iNOS expression in **e** Tl(I)- or **f** Tl(III)-treated cells. Dotted lines show the 95% confidence band of the best fit-line. Results are show the mean ± SEM ($n \geq 3$). *Asterisk* denotes a statistical significance respect to the value measured in control cells ($P < 0.05$)

Effects on SOD and CAT

Cytosolic (CuZnSOD) and mitochondrial (MnSOD) isoforms of SOD were analyzed, as they generate H_2O_2 that could oxidize DHR123. At 10 µM Tl(I), increased expression of CuZnSOD was observed ($P < 0.05$ vs. controls), with decreased expression for the remaining concentrations assessed ($P < 0.05$ vs. controls; Fig. 4a, b). Tl(III) decreased CuZnSOD expression levels (Fig. 4a, b) in a concentration-dependent manner ($P < 0.01$ vs. controls). However, CuZnSOD activity remained within control values for all the experimental situations assessed (Fig. 4c). Tl(I) and Tl(III) had opposed effects on MnSOD expression and activity. Tl(I) increased significantly MnSOD expression ($P < 0.05$ vs. controls; Fig. 4d, e), followed by 47 and 30% increase in its activity at 10 and 25 µM concentration, respectively (Fig. 4F). In contrast, Tl(III) decreased both MnSOD expression ($P < 0.005$ vs. controls; Fig. 4d, e) and activity ($P < 0.05$ vs. controls; Fig. 4f) in a concentration-dependent manner.

We next evaluated the impact of Tl exposure on CAT expression, one of the enzymes that metabolize H_2O_2. After 6 h of incubation, Tl(I) or Tl(III) caused no significant changes in CAT expression levels (Fig. 5a, b). Although,

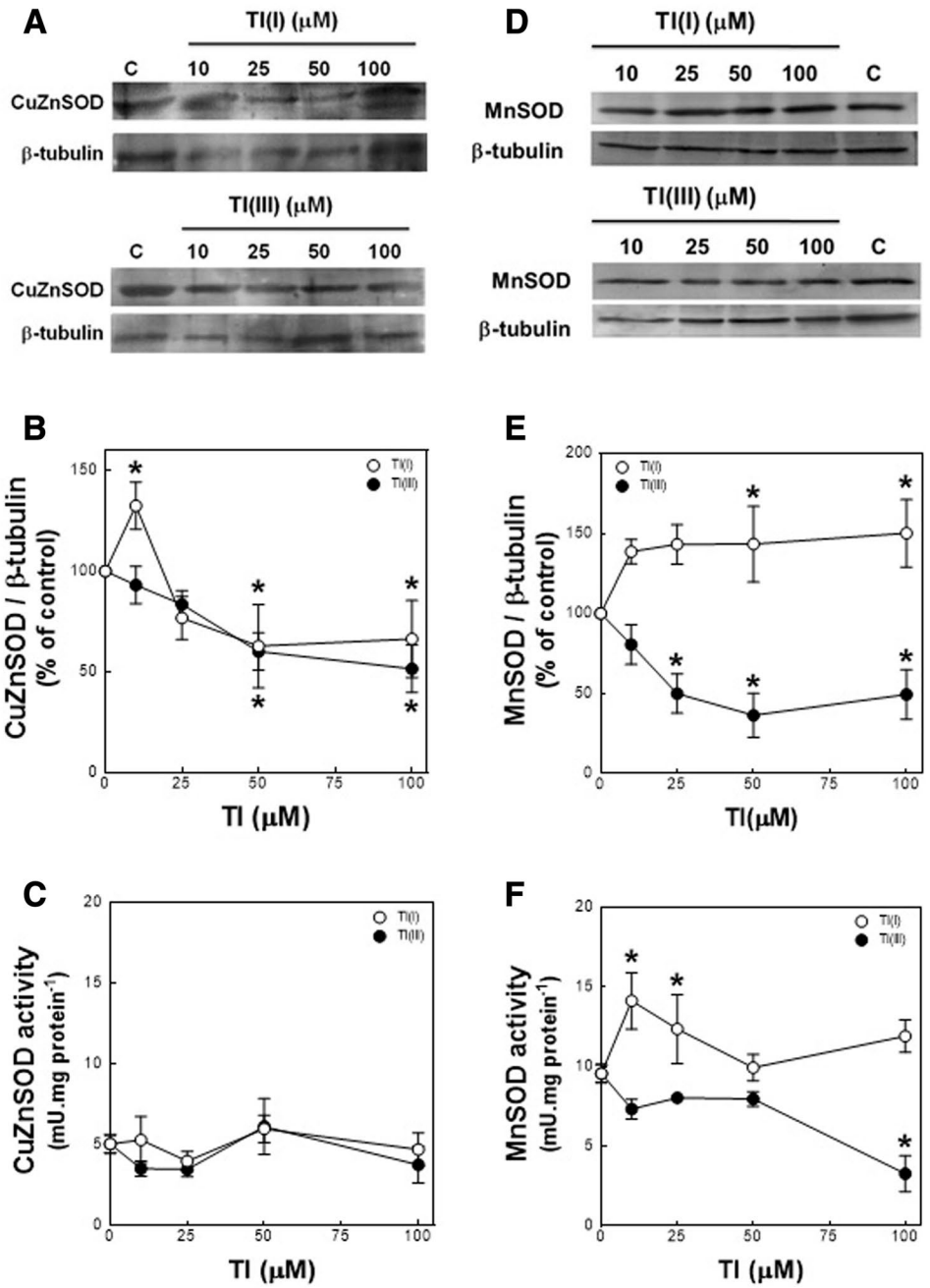

Fig. 4 Tl(I) and Tl(III) affected differently CuZnSOD and MnSOD expression and activities. PC12adh cells were incubated at 37 °C for 6 h in the presence of 10–100 µM Tl(I) or Tl(III). CuZnSOD and MnSOD expression and activities were evaluated. **a**, **d** Representative Western blots. Quantification of **b** CuZnSOD and **e** MnSOD to β-tubulin expression ratio in Tl(I) (*open circle*)- and Tl(III) (*filled circle*)-treated cells. Activities of **(C)** CuZnSOD and **f** MnSOD measured in Tl(I) (*open circle*)- and Tl(III) (*filled circle*)-treated cells, expressed as the percentage of the value recorded in control cells. Results are shown as the mean ± SEM ($n \geq 3$). *Asterisk* denotes a statistical significance respect to the value measured in control cells ($P < 0.01$)

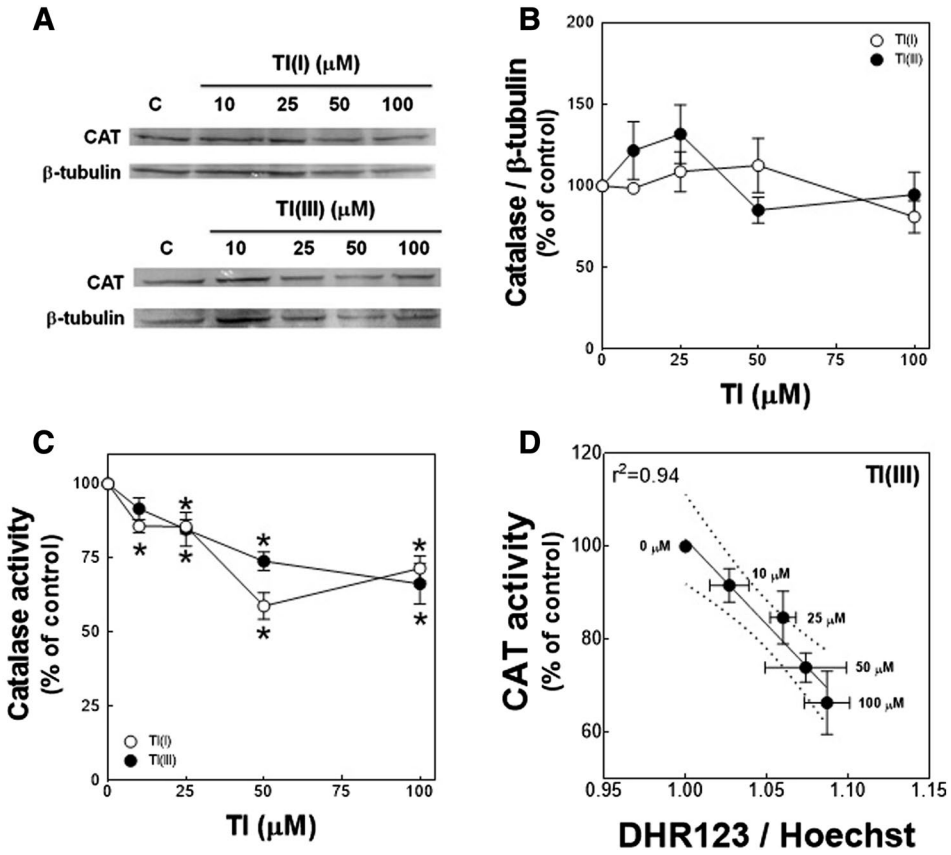

Fig. 5 Tl decreased CAT activity without affecting its expression. PC12adh cells were incubated at 37 °C for 6 h in the presence of 10–100 μM Tl(I) or Tl(III). CAT expression and activity were evaluated. **a** Representative Western blots. **b** Quantification of CAT to β-tubulin expression ratio in Tl(I) (*open circle*)- and Tl(III) (*filled circle*)-treated cells. **c** CAT activity measured in Tl(I) (*open circle*)- and Tl(III) (*filled circle*)-treated cells, expressed as the percentage of the data obtained in control cells. **d** Correlation between CAT activity and maximal Tl(III)-mediated DHR123 oxidation. Dotted lines show the 95% confidence band of the best fit-line. Results are shown as the mean ± SEM ($n \geq 3$). *Asterisk* denotes a statistical significance respect to the value measured in control cells ($P < 0.01$)

both cations decreased CAT activity to a similar extent and in a concentration-dependent manner ($P < 0.005$ vs. controls; Fig. 5c). A negative correlation ($r^2 = 0.94$, $P < 0.01$) was found between maximal oxidant production in Tl(III)-treated cells and remnant CAT activity (Fig. 5d).

Effects on glutathione-dependent system

In addition to CAT, H_2O_2 is also metabolized by the GSH-dependent antioxidant defense system. Up to 50 μM, Tl(I) did not affect GSH content (Fig. 6a), but at 100 μM Tl(I), GSH content decreased in a time-dependent manner ($P < 0.001$ vs. controls). Tl(III) did not affect GSH content, regardless its concentration or the exposure time assessed (Fig. 6b). These results suggest that GSH will not limit the extent of H_2O_2 reduction in Tl-treated cells.

The expression and activity of the enzyme GPx were next evaluated. In Tl(I) (10–100 μM)-treated cells no significant changes were observed in GPx-1/2 expression (Fig. 7a, b). In contrast, 25 and 50 μM Tl(III) increased its expression in 82 and 54%, respectively ($P < 0.01$ vs. controls; Fig. 7b). Total GPx activity displayed a biphasic behavior (Fig. 7c). At 10 μM, Tl(I) and Tl(III) decreased GPx activity in 44 and 25%, respectively ($P < 0.01$ vs. controls). At higher concentrations, Tl(I) did not affect GPx activity while Tl(III) increased it in a concentration-dependent manner (90% at 100 μM concentration; $P < 0.01$ vs. controls). A significant, positive correlation was found between maximal DHR123 oxidation achieved in Tl(III)-treated cells and GPx activity ($P < 0.01$; Fig. 7d).

Tl(I) and Tl(III) decreased GR expression (Fig. 8a, b). The magnitude of the effect in Tl(I)-treated cells ranged from 40 to 57%, but no clear relationship with metal concentration was found. In contrast, Tl(III) decreased GR expression in a concentration-dependent manner, reaching 60% lower values at 100 μM (Fig. 8b). In the 25–100 μM range of concentrations, the Tl(I) and Tl(III) had similar effects on GR expression. While GR activity in Tl(I)-exposed cells remained within control values (Fig. 8c), it was increased in Tl(III) (10–50 μM)-treated cells ($P < 0.05$ vs. controls). However, at 100 μM Tl(III), GR activity was comparable to those in the controls.

Effects on thioredoxin-dependent system

H_2O_2 can also be metabolized by the Trx-dependent system. In Tl(I)-exposed cells a significant increase in the expression of 2-Cys Prx (isoforms 1, 2 and 4) was observed ($P < 0.005$ *vs.* controls; Fig. 9a, b), reaching a maximum at 50 μM Tl(I). In addition, a tendency towards increased 2-Cys Prx activity was observed in these cells, reaching the maximal activity at 50 μM ($P < 0.05$ vs. controls; Fig. 9c). In contrast, the

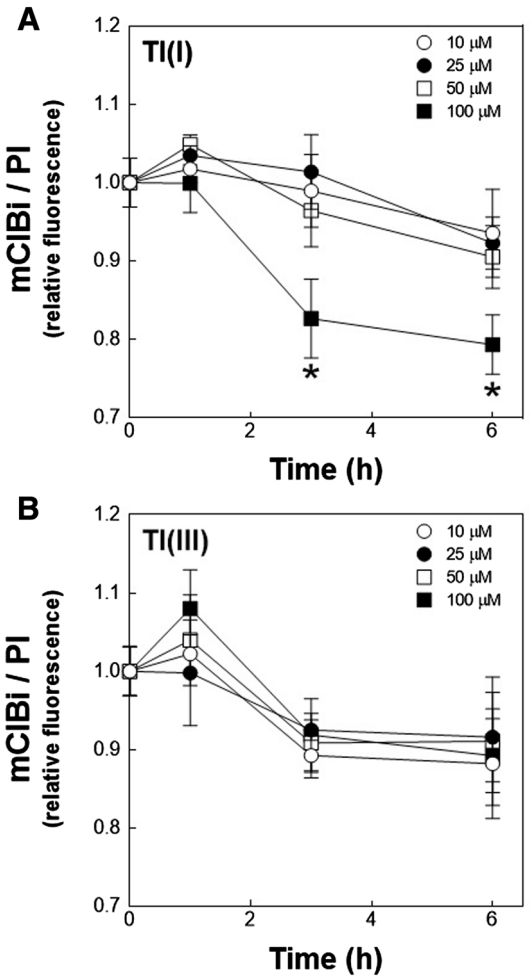

Fig. 6 Tl(I) (100 µM) caused a rapid decrease in GSH content. PC12adh cells were incubated at 37 °C for 1–6 h to 10 µM (*open circle*), 25 µM (*filled circle*), 50 µM (*open square*) or 100 µM (*filled square*) **a** Tl(I) or **b** Tl(III). GSH content was evaluated in the samples from the reaction with monochlorobimane (mClBi), and data were normalized by DNA content measured with PI. Results are shown as the mean ± SEM ($n = 3$). *Asterisk* denotes a statistical significance respect to the value measured in control cells ($P < 0.01$)

expression (Fig. 9a, b) and activity (Fig. 9c) of 2-Cys Prx in Tl(III)-treated cells remained within control values for all the concentrations assessed.

Finally, the effects of Tl(I) and Tl(III) on TrxR expression and activity were evaluated. Tl(I) significantly increased TrxR1 expression ($P < 0.001$ vs. controls; Fig. 10a, b) and decreased TrxR2 expression ($P < 0.01$ vs. controls; Fig. 10a, b) in a concentration-dependent manner. The effect of Tl(III) on TrxR1 was biphasic, increasing its expression significantly at 25 µM and restoring to basal levels at higher concentrations (Fig. 10a, b). A tendency towards increased expression of TrxR2 was observed in 100 µM Tl(III)-treated cells ($P = 0.09$ vs. controls; Fig. 10a, c). The activity of TrxR measured in 100 µM Tl(I)-treated cells was 32% higher than in the controls ($P < 0.05$; Fig. 10d). Like the observed for GR, Tl(III) increased markedly TrxR activity ($P < 0.01$ vs. controls; Fig. 10d). Significant, positive correlations were found between maximal oxidant production and TrxR activity for cells treated with Tl(I) ($r^2 = 0.96$, $P < 0.01$; Fig. 10e) or Tl(III) ($r^2 = 0.97$, $P < 0.01$; Fig. 10f).

Discussion

Exacerbated ROS production is a common mechanism in heavy metal toxicity (Jomova and Valko 2011). Increased ROS production by Tl(I) was first described by Hasan and Ali (1981) who administered Tl(I) acetate (5 mg/kg ip) to rats and observed the accumulation of lipid peroxidation products in the brain, brain stem and cerebellum. Similar results were observed after the subchronic administration of Tl(I) acetate to rats, in doses equivalent to 1/20 and 1/40 of median lethal dose (Galván-Arzate et al. 2000). Studies performed in cultured cells or isolated mitochondria indicate that these organelles are main targets of Tl toxicity (Korotkov and Brailovskaya 2001; Korotkov and Lapin 2003; Hanzel and Verstraeten 2006; Pourahmad et al. 2010). In traditional, poorly adherent PC12 cells, both Tl(I) and Tl(III) increase H_2O_2 production with kinetics that have two maximums, at 1 and 24 h of exposure to Tl, respectively. The second event occurs after the onset of mitochondria depolarization, around ~18 h of cell exposure to Tl (Hanzel and Verstraeten 2006). In the present work, we extended those studies, investigating if the newly generated adherent variant of PC12 (PC12adh) cells also had increased ROS/RNS production upon Tl exposure, and the manner that they managed oxidant excess through the modulation of the enzymes that constitute the antioxidant defense system.

First, the impact of Tl(I) and Tl(III) on cell viability and oxidant production were verified in the current model. In living cells, MTT is metabolized by succinate dehydrogenase complex (E.C. 1.3.99.1) which is involved in mitochondrial electron transfer chain. Therefore, this method evaluates the presence of cells with preserved mitochondrial functionality. Until 6 h of cell exposure to Tl(I) or Tl(III) (10–100 µM) more than 95% of cells had preserved mitochondria. This result was confirmed analyzing the uptake of Neutral red by cells with preserved lysosomal functionality. The maintenance of cell viability throughout the experiment was crucial for the subsequent determinations that rely on cell capacity to synthesize and maintain enzyme functionality.

Oxidant production was evaluated using DHR123 which is oxidized in the intracellular milieu to rhodamine 123. The kinetics of oxidant generation depended on the time of cell exposure to the cations. The time necessary to reach maximal oxidant generation (T_{max}), decreased exponentially with the concentration of Tl(I) but remained constant

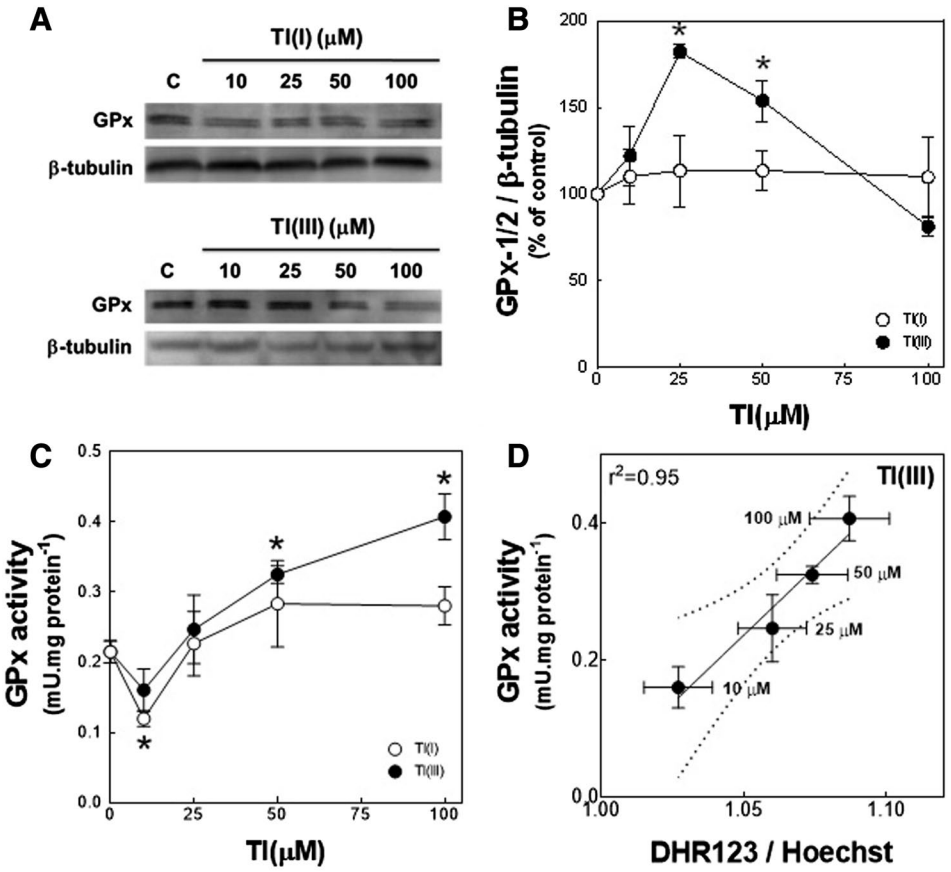

Fig. 7 Tl(lll) (25–50 μM) increased GPx-1/2 expression and its activity correlated positively with maximal oxidant production. PC12adh cells were incubated at 37 °C for 6 h in the presence of 10–100 μM Tl(I) or Tl(III) and GPx-1/2 expression and activity were evaluated. **a** Representative Western blots. **b** Quantification of GPx-1/2 to β-tubulin expression ratio in Tl(I) (*open circle*)- and Tl(III) (*filled circle*)-treated cells. **c** Total GPx activity was measured in Tl(I) (*open circle*)- and Tl(III) (*filled circle*)-treated cells and data were expressed as the percentage of the value recorded in control cells. **d** Correlation between total GPx activity and maximal Tl(III)-mediated DHR123 oxidation. *Dotted lines* show the 95% confidence band of the best fit-line. Results are shown as the mean ± SEM ($n = 3$). *Asterisk* denotes a statistical significance respect to the value measured in control cells ($P < 0.001$)

in Tl(III)-exposed cells, peaking around 0.5–1 h of incubation regardless the concentration of the cation assessed. The different velocities in the production of oxidants could be related to the fact that these cations do not share common transporters in the cells, or to dissimilar toxic potential. One of the routes used by Tl(III) to enter PC12 cells is the internalization of Tl(III)-transferrin complex via endosomes (Hanzel et al. 2012). On the other hand, as Tl(I) resembles K^+ in its ionic radius and charge, it uses K^+ transporters—e.g. Na^+/K^+-ATPase and/or Na^+, K^+, Cl^- cotransporter—to enter cells (Brismar et al. 1995; Sherstobitov et al. 2010). Regardless the mechanisms involved in Tl entry, obtained results suggest that Tl(III) could be more toxic than Tl(I) to PC12adh cells because, at the same extracellular concentration, Tl(III) affected cell redox status faster than Tl(I).

DHR123 detects not only H_2O_2 but also peroxynitrite anion ($ONOO^{\cdot-}$) (Crow 1997). However, we expected the contribution of the latter to be minimal, as non-differentiated PC12 cells express low amounts of NOS (Peunova and Enikolopov 1995; Nakagawa et al. 2000). This was true for nNOS, but we found that even non-stimulated PC12adh cells expressed iNOS and that its expression was increased by 10–50 μM Tl(I) or Tl(III). In addition, iNOS expression levels correlated positively with the content of nitrite released to the media, pointing to iNOS as the source of nitrite observed. As NO and $O_2^{\cdot-}$ generate $ONOO^{\cdot-}$ in a non-enzymatic reaction, both substrates must be formed simultaneously. The source of $O_2^{\cdot-}$ could not be plasma membrane-associated NOX, as Tl did not affect its activity throughout the period investigated (0.5 to 6 h). In addition, no inhibition of CuZnSOD activity that could account for transient $O_2^{\cdot-}$ increase was evidenced. However, we cannot discard other sources of $O_2^{\cdot-}$ generation, such as mitochondrial respiratory chain. In fact, the expression and activity of mitochondrial MnSOD were decreased in Tl(III)-exposed cells that would increase $O_2^{\cdot-}$. In contrast, Tl(I) increased the expression and activity of this enzyme, and thus once generated, $O_2^{\cdot-}$ proceeds to H_2O_2. Hence, in Tl(I)-treated cells the oxidant species detected by DHR123 would be mostly H_2O_2, while in Tl(III)-treated cells they would be both H_2O_2 and $ONOO^{\cdot-}$.

We observed that, once reached a maximum, DHR123 oxidation decreased towards a steady-state value slightly higher than before treatment. Thus, we hypothesized that cells counterbalanced oxidant species production through the activation and/or increased expression of the enzymes responsible for oxidant metabolization. Three main enzymatic systems could metabolize H_2O_2: CAT, GSH- and Trx-dependent systems. In addition, $ONOO^{\cdot-}$ can be metabolized

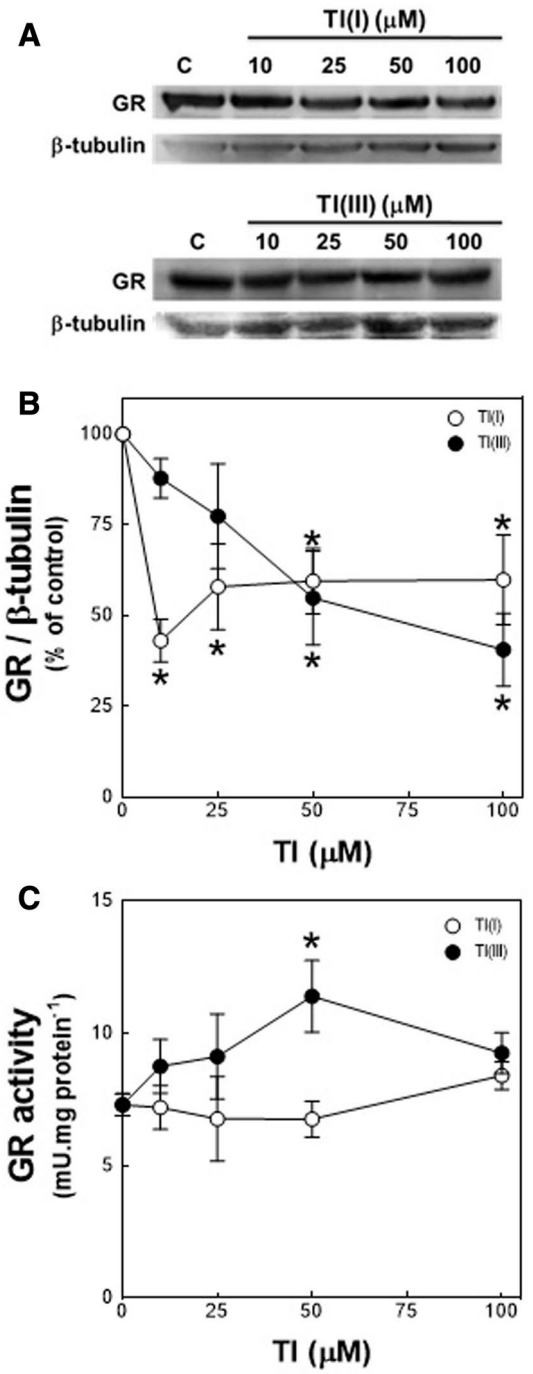

Fig. 8 Tl reduced GR expression although its activity was unaltered or even increased. PC12adh cells were incubated at 37 °C for 6 h in the presence of 10–100 μM Tl(I) or Tl(III) and GR expression and activity were evaluated. **a** Representative Western blots. **b** Quantification of GR to β-tubulin expression ratio in Tl(I) (*open circle*)- and Tl(III) (*filled circle*)-treated cells. **c** GR activity measured in Tl(I) (*open circle*)- and Tl(III) (*filled circle*)-treated cells, expressed as the percentage of the value recorded in control cells. Results are shown as the mean ± SEM ($n \geq 3$). *Asterisk* denotes a statistical significance respect to the value measured in control cells ($P < 0.05$)

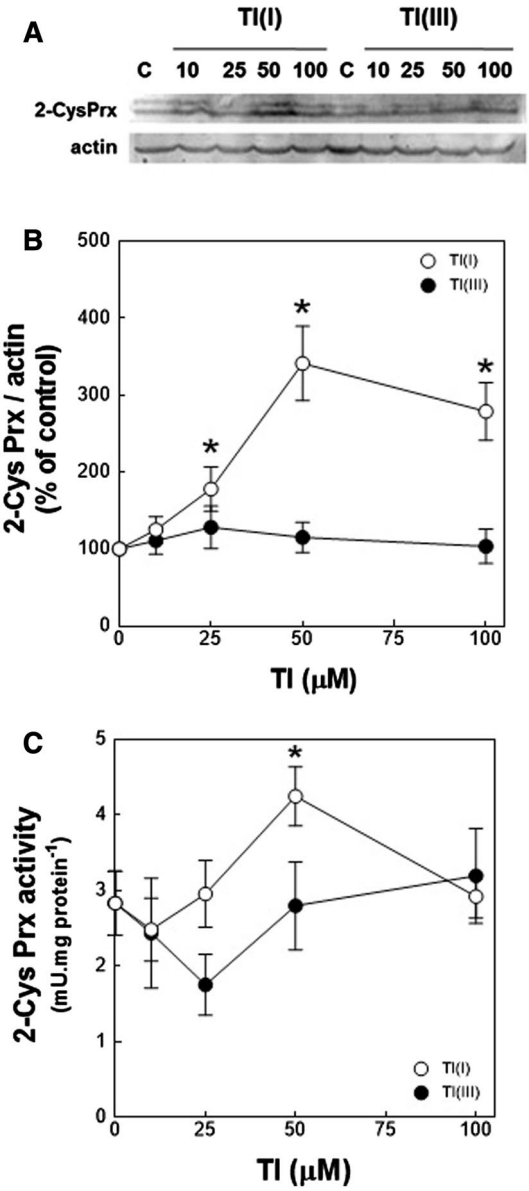

Fig. 9 Tl(I) increased 2-Cys Prx expression and activity. PC12adh cells were incubated at 37 °C for 6 h in the presence of 10–100 μM Tl(I) or Tl(III) and 2-Cys Prx expression and activity were evaluated. **a** Representative Western blots. **b** Quantification of 2-Cys Prx to actin expression ratio in Tl(I) (*open circle*)- and Tl(III) (*filled circle*)-treated cells. **c** Two-Cys Prx activity measured in Tl(I) (*open circle*)- and Tl(III) (*filled circle*)-treated cells, and expressed as the percentage of the value recorded in control cells. Results are shown as the mean ± SEM ($n = 4$). *Asterisk* denotes a statistical significance respect to the value measured in control cells ($P < 0.005$)

by GPx-1 (Speckmann et al. 2016) present in mitochondria and cytosol of most cell types (Rhee et al. 2005).

In Tl-exposed cells, no alterations in CAT expression were observed after 6 h of incubation. However, both cations markedly reduced its activity in concentration-dependent manners. In fact, CAT activity in Tl(III)-treated cells

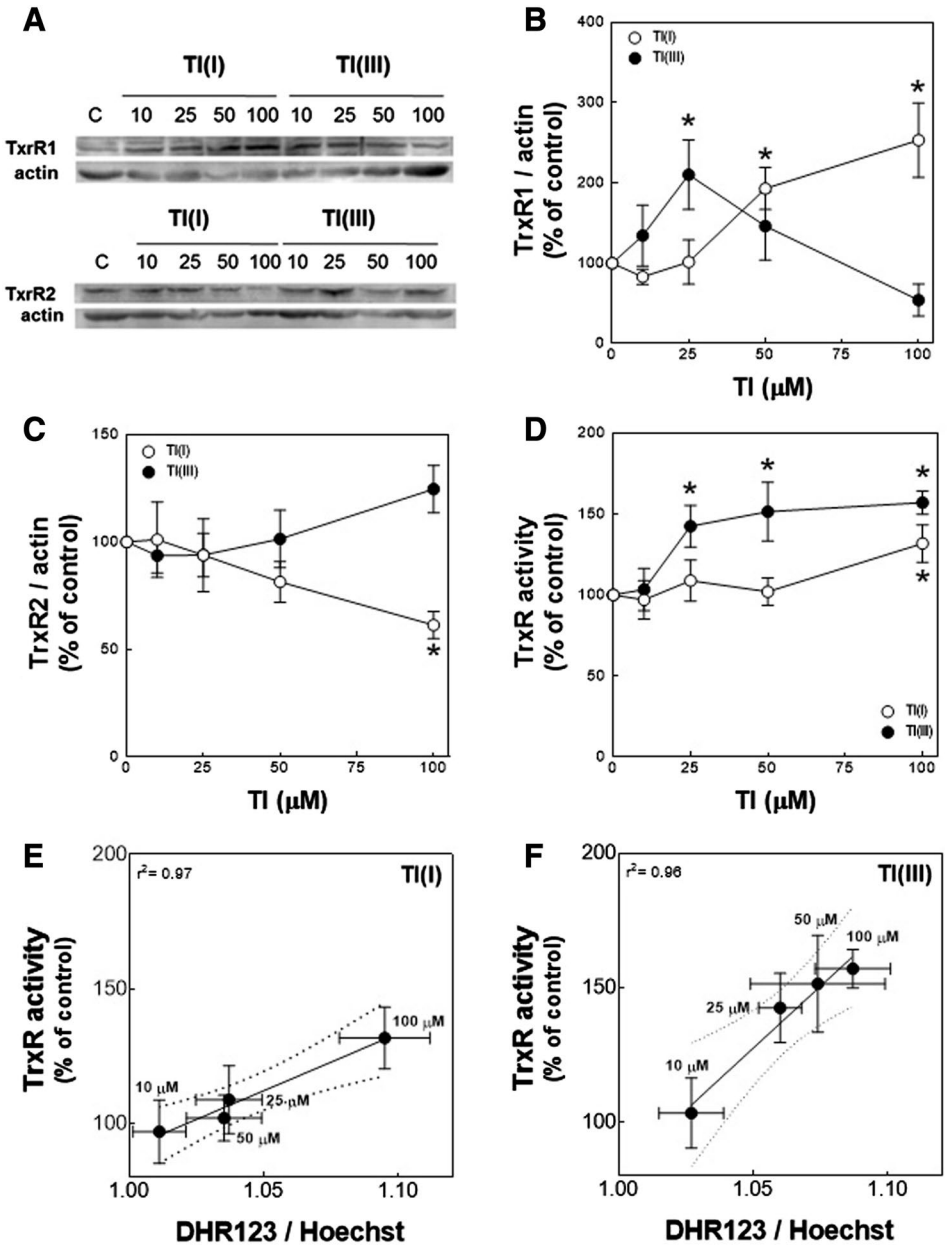

Fig. 10 Tl affected TrxR expression and its activity correlated positively with maximal oxidant production. PC12adh cells were incubated at 37 °C for 6 h in the presence of 10–100 μM Tl(I) or Tl(III) and TrxR1 and TrxR2 expression were evaluated. **a** Representative Western blots. Quantification of **b** TrxR1 and **c** TrxR2 to actin expression ratio in Tl(I) (*open circle*)- and Tl(III) (*filled circle*)-treated cells. **d** Total TrxR activity measured in Tl(I) (*open circle*)- and Tl(III) (*filled circle*)-treated cells, expressed as the percentage of the value recorded in control cells. Correlations between TrxR activity and maximal **e** Tl(I)- and **f** Tl(III)-mediated DHR123 oxidation. *Dotted lines* show the 95% confidence band of the best fit-line. Results are shown the mean ± SEM ($n \geq 3$). *Asterisk* denotes a statistical significance respect to the value measured in control cells ($P < 0.001$)

correlated negatively with oxidant generation, a relationship that was less marked ($r^2 = 0.72$, $P = 0.07$; correlation not shown) in Tl(I)-treated cells. Both ROS and RNS can modulate CAT activity. As CAT can be inhibited by $O_2^{\cdot-}$ (Shimizu et al. 1984), impaired $O_2^{\cdot-}$ removal by MnSOD in Tl(III)-treated cells could partially account for CAT inhibition. In contrast, MnSOD and CuSOD activities were preserved or even increased in Tl(I)-exposed cells, and $O_2^{\cdot-}$-mediated CAT inhibition would not occur. Alternatively, CAT activation can be prevented by H_2O_2 excess which avoids CAT phosphorylation in Tyr231 and Tyr386 (Rhee et al. 2005), leading to further H_2O_2 accumulation. Finally, CAT can be inhibited in vitro by $ONOO^{-}$ (Grzelak et al. 2000). Hence, all these three inhibitory mechanisms could be operative in Tl(III)-treated cells, aggravating the oxidative stress caused by this cation.

We reported previously that after 24 h of incubation, Tl(I) and Tl(III) decreased GSH content in PC12 cells (Hanzel and Verstraeten 2006). On this basis, we investigated if this could be an initial event that leads to an impairment of GSH-dependent system. While no significant variations in GSH content were observed in Tl(III)-treated cells up to 6 h of cell exposure to the cation, a marked and time-dependent GSH decrease was found in cells treated with 100 μM Tl(I). However, considering that the maximal effect measured corresponded to a ~20% decrease and that the cellular concentration of GSH lays in the millimolar order, it is unlikely that GSH-dependent system would be impaired by the exhaustion

of its co-substrate. However, prolonged exposure to the cations would decrease the functionality of the system with the consequent accumulation of H_2O_2 (Hanzel and Verstraeten 2006).

Non-differentiated PC12 cells express both GPx-1 (Wang et al. 2009) and GPx-2 (Ciofani et al. 2014) present in cytosol, nuclei and mitochondria. No significant alterations in GPx-1/2 expression and activity were evidenced in cells exposed to Tl(I), but both parameters were increased in Tl(III)-treated cells. In fact, GPx activity at 6 h of treatment correlated positively with oxidant species production at 30 min. This finding suggests that GPx activity could be increased as a response against the initial insult of H_2O_2 and/or $ONOO^{-}$ (Speckmann et al. 2016). Worth of noticing, GPx-1/2 expression in cells exposed to 100 µM Tl(III) remained within control values although its activity was markedly increased. GPx can be activated upon phosphorylation in Tyr96 in response to increased H_2O_2 (Rhee et al. 2005), conciliating the discrepancy between the expression levels and functionality. In vitro, Tl(I) and Tl(III) interact with GPx causing its inactivation (Villaverde et al. 2004). Therefore, GPx activity measured in Tl-exposed cells could be the resultant between increased activity in response to the oxidative insult, and the inhibition due to Tl-enzyme interaction. Nevertheless, increased GPx activity in Tl(III)-exposed cells could be an early mechanism to decrease H_2O_2 and/or $ONOO^{-}$ levels to physiological values.

Along with peroxide reduction by GPx, GSH is oxidized to GSSG, GR being the enzyme responsible for its recycling. Although GR expression was reduced in Tl(I)- and Tl(III)-treated cells, its activity remained unaltered or even increased. To the best of our knowledge, GR had no post-translational regulatory mechanisms that conceal these apparently contradictory findings. In fact, direct interaction between Tl(I) and Tl(III) with purified GR causes its inhibition, especially with Tl(III) which impairs both reductase and diaphorase activities of GR (Villaverde et al. 2004). This raises the possibility of a methodological pitfall in GR activity determination, that quantifies NADPH oxidation coupled to the enzymatic reduction of GSSG. In addition to GR, TrxR also uses NADPH to maintain Trx in its reduced, active form (Hanschmann et al. 2013). Thus, it is possible that both GR and TrxR activities were quantified simultaneously in the samples. Hence, TrxR activity was measured from Trx capacity to reduce insulin disulfide bridges, that cannot be mediated by GSH. As observed for GR, TrxR activity was either unaltered [Tl(I)] or increased [Tl(III)], supporting the hypothesis that the method used for GR activity measurement quantified simultaneously both enzymes.

TrxR expression was evaluated measuring the expression levels of the cytoplasmic (TrxR1) and mitochondrial (TrxR2) isoforms. Overall, Tl(I) and Tl(III) had opposed effects on TrxR1 and TrxR2 expression. Tl(I) increased TrxR1 expression in a concentration-dependent manner, while it decreased that of TrxR2. Worth of noticing, Tl(III) had a biphasic effect on TrxR1 expression, resembling those on iNOS and GPx expression. This observation raises the possibility that low concentrations of Tl(III) could induce common signaling pathway/s that ultimately regulate/s the expression of these enzymes, and this hypothesis is currently under investigation. In addition, Tl(III) caused mild increase of mitochondrial TrxR2 expression that could account for the increased TrxR activity measured at the highest concentrations of the cation.

Finally, the effects of Tl on 2-Cys Prx expression and activity were investigated. Prx are classified into 2-Cys Prx (Prx-1 to Prx-4), atypical 2-Cys Prx (Prx-5) and 1-Cys Prx (Prx-6) (Hanschmann et al. 2013), all of them being expressed in PC12 cells (Chen et al. 2007). Tl(I) increased 2.5-folds the expression of 2-Cys Prx, although their activity was not increased in the same magnitude (1.5-fold at 50 µM concentration). The increased expression of 2-Cys Prx in Tl(I)-treated cells coincides with the decreased concentration of GSH, which was also observed in PC12 cells submitted to different stimuli (Simzar et al. 2000), suggesting that 2-Cys Prx may regulate GSH-dependent pathway. On the other hand, Tl(III) did not affect 2-Cys Prx expression levels, with activities that were within control values or even slightly decreased. Under oxidative stress conditions, the Cys in the active site of 2-Cys Prx can be oxidized by H_2O_2 (Rabilloud et al. 2002; Wagner et al. 2002; Yang et al. 2002), impairing its activity. Mildly decreased Prx activity observed in Tl(III)-exposed cells aggravates their oxidative stress status, as Prx-2 reduces not only H_2O_2 but also $ONOO^{-}$ (Manta et al. 2009).

In summary, obtained results indicate that, similarly to the observed in the parental PC12 cell line, both Tl(I) and Tl(III) cause a rapid increase in oxidant species production in PC12adh cells. This effect is counterbalanced by increasing the expression and/or activity of the enzymatic antioxidant defense system. In the case of cells treated with Tl(I), the main oxidant generated seems to be H_2O_2, which was metabolized mostly through the Trx-dependent system. On the other hand, Tl(III) increased both H_2O_2 and $ONOO^{-}$, which were eliminated via the GSH- and Trx-dependent systems. Although this early oxidative insult imposed by the cations was almost normalized after 6 h, prolonged exposures to the cations could result in mitochondrial damage associated with a second wave of oxidant generation, that ultimately leads to the promotion of cell death by apoptosis (Hanzel and Verstraeten 2006, 2009).

Acknowledgements This work was supported by grants of the University of Buenos Aires (B086 and 20020100100112) and Agencia Nacional de Promoción Científica y Tecnológica (ANPCyT; PICT2013-1018). SVV is a career investigator of the CONICET (National Research Council, Argentina). LCPM was a recipient of

an undergraduate fellowship from the University of Buenos Aires (Argentina).

Compliance with ethical standards

Conflict of interest The authors declare no conflicts of interest.

References

ATSDR (1999) Thallium. ATSDR (Agency for Toxic Substances and Disease Registry). Prepared by Clement International Corp., under contract 205-88-0608, Atlanta, GA

Bradford MM (1976) A rapid and sensitive method for the quantitation of microgram quantities of protein utilizing the principle of protein-dye binding. Anal Biochem 72:248–254

Brismar T, Anderson S, Collins VP (1995) Mechanism of high K^+ and Tl^+ uptake in cultured human glioma cells. Cell Mol Neurobiol 15(3):351–360

Castilho RF, Ward MW, Nicholls DG (1999) Oxidative stress, mitochondrial function, and acute glutamate excitotoxicity in cultured cerebellar granule cells. J Neurochem 72(4):1394–1401

Chae HZ, Kim HJ, Kang SW, Rhee SG (1999) Characterization of three isoforms of mammalian peroxiredoxin that reduce peroxides in the presence of thioredoxin. Diabetes Res Clin Pract 45(2–3):101–112

Chen HM, Lee YC, Huang CL et al (2007) Methamphetamine downregulates peroxiredoxins in rat pheochromocytoma cells. Biochem Biophys Res Commun 354(1):96–101

Ciofani G, Genchi GG, Mazzolai B, Mattoli V (2014) Transcriptional profile of genes involved in oxidative stress and antioxidant defense in PC12 cells following treatment with cerium oxide nanoparticles. Biochim Biophys Acta 1840(1):495–506

Crow JP (1997) Dichlorodihydrofluorescein and dihydrorhodamine 123 are sensitive indicators of peroxynitrite in vitro: implications for intracellular measurement of reactive nitrogen and oxygen species. Nitric Oxide 1(2):145–157

Dringen R, Kussmaul L, Hamprecht B (1998) Detoxification of exogenous hydrogen peroxide and organic hydroperoxides by cultured astroglial cells assessed by microtiter plate assay. Brain Res Protoc 2(3):223–228

Galvan-Arzate S, Rios C (1994) Thallium distribution in organs and brain regions of developing rats. Toxicology 90(1–2):63–69

Galván-Arzate S, Martínez A, Medina E, Santamaría A, Ríos C (2000) Subchronic administration of sublethal doses of thallium to rats: effects on distribution and lipid peroxidation in brain regions. Toxicol Lett 116:37–43

Grzelak A, Soszynski M, Bartosz G (2000) Inactivation of antioxidant enzymes by peroxynitrite. Scand J Clin Lab Invest 60(4):253–258

Guevara I, Iwanejko J, Dembinska-Kiec A et al (1998) Determination of nitrite/nitrate in human biological material by the simple Griess reaction. Clin Chim Acta 274(2):177–188

Halliwell B, Gutteridge J (1999) Free radicals in biology and medicine, 3rd edn. Oxford University Press, New York

Hanschmann EM, Godoy JR, Berndt C, Hudemann C, Lillig CH (2013) Thioredoxins, glutaredoxins, and peroxiredoxins–molecular mechanisms and health significance: from cofactors to antioxidants to redox signaling. Antioxid Redox Signal 19(13):1539–1605

Hanzel CE, Verstraeten SV (2006) Thallium induces hydrogen peroxide generation by impairing mitochondrial function. Toxicol Appl Pharmacol 216(3):485–492

Hanzel CE, Verstraeten SV (2009) Tl(I) and Tl(III) activate both mitochondrial and extrinsic pathways of apoptosis in rat pheochromocytoma (PC12) cells. Toxicol Appl Pharmacol 236(1):59–70

Hanzel CE, Almeira Gubiani MF, Verstraeten SV (2012) Endosomes and lysosomes are involved in early steps of Tl(III)-mediated apoptosis in rat pheochromocytoma (PC12) cells. Arch Toxicol 86(11):1667–1680

Hasan M, Ali SF (1981) Effects of thallium, nickel, and cobalt administration of the lipid peroxidation in different regions of the rat brain. Toxicol Appl Pharmacol 57(1):8–13

Holmgren A, Bjornstedt M (1995) Thioredoxin and thioredoxin reductase. Methods Enzymol 252:199–208

Johansson LH, Borg LA (1988) A spectrophotometric method for determination of catalase activity in small tissue samples. Anal Biochem 174(1):331–336

Jomova K, Valko M (2011) Advances in metal-induced oxidative stress and human disease. Toxicology 283(2–3):65–87

Kim JA, Park S, Kim K, Rhee SG, Kang SW (2005) Activity assay of mammalian 2-cys peroxiredoxins using yeast thioredoxin reductase system. Anal Biochem 338(2):216–223

Korotkov SM, Brailovskaya LV (2001) Tl^+ increases the permeability of the inner membranes of rat liver mitochondria for monovalent cations. Dokl Biochem Biophys 378:145–149

Korotkov SM, Lapin AV (2003) Thallium induces opening of the mitochondrial permeability transition pore in the inner membrane of rat liver mitochondria. Dokl Biochem Biophys 392:247–252

Lu J, Holmgren A (2014) The thioredoxin antioxidant system. Free Radic Biol Med 66:75–87

Manta B, Hugo M, Ortiz C, Ferrer-Sueta G, Trujillo M, Denicola A (2009) The peroxidase and peroxynitrite reductase activity of human erythrocyte peroxiredoxin 2. Arch Biochem Biophys 484(2):146–154

Mosmann T (1983) Rapid colorimetric assay for cellular growth and survival: application to proliferation and cytotoxicity assays. J Immunol Methods 65(1–2):55–63

Nakagawa H, Yoshida M, Miyamoto S (2000) Nitric oxide underlies the differentiation of PC12 cells induced by depolarization with high KCl. J Biochem 127(1):113–119

Ogusucu R, Rettori D, Munhoz DC, Netto LE, Augusto O (2007) Reactions of yeast thioredoxin peroxidases I and II with hydrogen peroxide and peroxynitrite: rate constants by competitive kinetics. Free Radic Biol Med 42(3):326–334

Peter AL, Viraraghavan T (2005) Thallium: a review of public health and environmental concerns. Environ Int 31(4):493–501

Peunova N, Enikolopov G (1995) Nitric oxide triggers a switch to growth arrest during differentiation of neuronal cells. Nature 375(6526):68–73

Pino MT, Marotte C, Verstraeten SV (2017) Epidermal growth factor prevents thallium(I)- and thallium(III)-mediated rat pheochromocytoma (PC12) cell apoptosis. Arch Toxicol 91(3):1157–1174

Pourahmad J, Eskandari MR, Daraei B (2010) A comparison of hepatocyte cytotoxic mechanisms for thallium (I) and thallium (III). Environ Toxicol 25(5):456–467

Rabilloud T, Heller M, Gasnier F et al (2002) Proteomics analysis of cellular response to oxidative stress. Evidence for in vivo overoxidation of peroxiredoxins at their active site. J Biol Chem 277(22):19396–19401

Repetto G, Del Peso A, Repetto M (1998) Human thallium toxicity. In: Nriagu J (ed) Thallium in the environment. Advances in environmental science and technology. Wiley, Hoboken, pp 167–199

Rhee SG, Yang KS, Kang SW, Woo HA, Chang TS (2005) Controlled elimination of intracellular H(2)O(2): regulation of peroxiredoxin, catalase, and glutathione peroxidase via post-translational modification. Antioxid Redox Signal 7(5–6):619–626

Sherstobitov AO, Lapin AV, Glazunov VV, Nikiforov AA (2010) Transport of monovalent thallium across the membrane of oocyte of the lamprey *Lampetra fluviatilis*. Zh Evol Biokhim Fiziol 46(3):198–202

Shimizu N, Kobayashi K, Hayashi K (1984) The reaction of superoxide radical with catalase. Mechanism of the inhibition of catalase by superoxide radical. J Biol Chem 259(7):4414–4418

Simzar S, Ellyin R, Shau H, Sarafian TA (2000) Contrasting antioxidant and cytotoxic effects of peroxiredoxin I and II in PC12 and NIH3T3 cells. Neurochem Res 25(12):1613–1621

Speckmann B, Steinbrenner H, Grune T, Klotz LO (2016) Peroxynitrite: from interception to signaling. Arch Biochem Biophys 595:153–160

Sun Y, Oberley LW, Li Y (1988) A simple method for clinical assay of superoxide dismutase. Clin Chem 34(3):497–500

Villaverde MS, Hanzel CE, Verstraeten SV (2004) In vitro interactions of thallium with components of the glutathione-dependent antioxidant defence system. Free Radic Res 38(9):977–984

Wagner E, Luche S, Penna L et al (2002) A method for detection of overoxidation of cysteines: peroxiredoxins are oxidized in vivo at the active-site cysteine during oxidative stress. Biochem J 366(Pt 3):777–785

Wang J, Rahman MF, Duhart HM et al (2009) Expression changes of dopaminergic system-related genes in PC12 cells induced by manganese, silver, or copper nanoparticles. Neurotoxicology 30(6):926–933

Wang W-L, Dai R, Yan H-W, Han C-N, Liu L-S, Duan X-H (2015) Current situation of PC12 cell use in neuronal injury study. Int J Biotechnol Well Ind 4(2):61–66

Wu G, Fang YZ, Yang S, Lupton JR, Turner ND (2004) Glutathione metabolism and its implications for health. J Nutr 134(3):489–492

Yang KS, Kang SW, Woo HA et al (2002) Inactivation of human peroxiredoxin I during catalysis as the result of the oxidation of the catalytic site cysteine to cysteine-sulfinic acid. J Biol Chem 277(41):38029–38036